pISSN 1598-2998, eISSN 2005-9256
https://doi.org/10.4143/crt.2025.333
Cancer Res Treat. 2025 Jun 18 [Epub ahead of print]

Original Article

NOVA1 Activation Modulates the Tumor Immune Microenvironment through STING Phosphorylation in Head and Neck Squamous Cell Carcinoma

Sehui Kim[1,2], **Hyang Mi Kim**[1], **Jae Min Bae**[3], **Sun Och Yoon**[1]

[1]Department of Pathology, Severance Hospital, Yonsei University College of Medicine, Seoul, [2]Department of Pathology, Korea University Guro Hospital, Seoul, [3]Yonsei University College of Medicine, Seoul, Korea

Purpose Neuro-oncological ventral antigen 1 (NOVA1), a neuron-specific pre-mRNA splicing factor, is involved in neuronal development and oncogenesis. NOVA1 overexpression is associated with favorable prognosis in head and neck squamous cell carcinoma (HNSCC) and gastric adenocarcinoma, whereas its downregulation correlates with poor outcomes. High NOVA1 levels in these cancers correlate with increased $CD3^+$ and $CD8^+$ T lymphocyte densities, suggesting involvement in tumor immune-inflammatory signals. This study explores NOVA1's role in regulating the immune-inflammatory cGAS-STING pathway in HNSCC cells and clinical tissues.

Materials and Methods HNSCC cell lines (FaDu, YD-10B, SNU-1066, and SNU-1076) were transfected with NOVA1 and poly(dA:dT). Quantitative real-time polymerase chain reaction and Western blot analysis were used to assess gene/protein expression. Enzyme-linked immunosorbent assay quantified cytokine levels, and immunoprecipitation assessed protein interactions. Clinical tissue samples from 234 HNSCC patients were analyzed using immunohistochemistry to correlate NOVA1 and STING pathway markers with immune cell infiltration.

Results NOVA1 overexpression in HNSCC cells increased phosphorylation of STING (p-STING) without altering cGAS or TBK1. Immunoprecipitation showed an interaction between NOVA1 and p-STING. Overexpression of NOVA1, particularly with poly(dA:dT) treatment, tended to elevate CCL5 and CXCL10 expression. In clinical samples, NOVA1 expression strongly correlated with p-STING levels ($r=0.749$, $p < 0.001$). Higher NOVA1 and p-STING expressions were linked to increased infiltration of $CD3^+$ T cells, $CD8^+$ T cells, and $FOXP3^+$ regulatory T cells.

Conclusion NOVA1 modulates the cGAS-STING pathway through STING phosphorylation and associated immune responses in HNSCC, providing a potential therapeutic target for enhancing anti-tumor immunity.

Key words NOVA1, cGAS-STING pathway, Squamous cell carcinoma, Head and neck, Tumor immunity

Introduction

Neuro-oncological ventral antigen 1 (NOVA1) is a neuron-specific pre-mRNA splicing factor that plays a crucial role in neuronal development. Beyond its neural functions, NOVA1 is also enriched in normal fibroblasts and activated T cells and is expressed in various cancers, suggesting its involvement in both normal cellular processes and tumor biology [1-4].

The cGAS-STING pathway is a key regulator of innate immunity and inflammation, implicated in autoimmune diseases, infections, and cancer [5]. In the context of tumor immunity, it plays a critical role in activating anti-tumor immune responses across multiple cancer types, such as melanoma, breast cancer, and head and neck squamous cell carcinoma (HNSCC) [6]. This pathway is initiated when cGAS senses cytosolic double-stranded DNA derived from pathogens or damaged host cells. Upon activation, cGAS synthesizes cyclic guanosine monophosphate (GMP)–adenosine monophosphate (AMP) (cGAMP), which binds to STING, inducing its oligomerization and translocation from the endoplasmic reticulum to the Golgi apparatus. At the Golgi, STING recruits and activates TANK-binding kinase 1 (TBK1). Activated TBK1 then phosphorylates STING, primarily at serine 366, a modification that is essential for the downstream activation of interferon regulatory factor 3 (IRF3) and nuclear factor-κB inhibitor IκBα. This signaling cascade leads to the induction of type I interferons and pro-inflammatory cytokines [6]. Critically, cGAS-STING activation drives the production of chemokines like C-C motif chemokine ligand 5 (CCL5) and C-X-C motif chemokine ligand 10 (CXCL10), which recruit immune cells such as $CD8^+$ cytotoxic T cells and natural killer cells into the tumor microenvironment, shaping anti-tumor immunity [5-10].

Phosphorylation of STING is a key post-translational modification that regulates its signaling function. As noted,

Correspondence: Sun Och Yoon
Department of Pathology, Yonsei University College of Medicine, Severance Hospital, 50-1 Yonsei-ro, Seodaemun-gu, Seoul 03722, Korea
Tel: 82-2-2228-1763 E-mail: soyoon@yuhs.ac
Received March 22, 2025 **Accepted** June 17, 2025

this phosphorylation occurs following cGAMP binding and STING translocation to the Golgi, where TBK1-mediated phosphorylation at serine 366 enables recruitment and activation of IRF3, leading to the transcription of interferon-stimulated genes [6]. Additionally, other kinases such as CSK (C-terminal Src kinase), EGFR (epidermal growth factor receptor), and SYK (spleen tyrosine kinase) are also involved in phosphorylating STING at different residues, impacting its activation and downstream signaling [11].

In our previous study, we found that NOVA1 overexpression is associated with better prognosis in patients with HNSCC and gastric adenocarcinoma, while reduced NOVA1 expression correlates with poorer outcomes. Tumors with high NOVA1 levels also show increased infiltration of $CD3^+$ and $CD8^+$ T lymphocytes, whereas tumors with low NOVA1 expression have reduced immune cell densities [12,13]. This suggests that NOVA1 may play a role in activating immune-inflammatory signals within the tumor microenvironment.

In our preliminary tests, RNA sequencing was performed on FaDu cells, a human HNSCC cell line, after treatment with poly(dA:dT) to assess NOVA1 gene expression. Differential gene expression and Kyoto Encyclopedia of Genes and Genomes (KEGG) pathway analyses revealed an upregulation of the cytokines *CCL5* and *CXCL10*, which are closely linked to the cGAS-STING signaling pathway (S1 Fig.). The cGAS-STING pathway plays a crucial role in inflammatory responses to infections, autoimmune diseases, and tumor immunity [7,8]. This suggests that NOVA1 may regulate immune-inflammatory signals in the tumor microenvironment through activation of the cGAS-STING pathway.

This study aims to clarify how NOVA1 regulates the cGAS-STING pathway in HNSCC. By examining NOVA1 expression *in vitro* and in clinical tissues, we seek to understand its role in tumor immune signaling. This could provide insights into immune activation within the tumor microenvironment and position NOVA1 as a potential therapeutic target to enhance anti-tumor immunity in HNSCC and other cancers.

Materials and Methods

1. Cell lines and culture conditions

The following human papillomavirus–negative HNSCC cell lines were used in this study: FaDu (ATCC HTB-43, pharyngeal squamous cell carcinoma [SCC]), SNU-1066 (01066, Korea Cell Line Bank [KCLB], laryngeal SCC), SNU-1076 (01076, KCLB, laryngeal SCC), and YD-10B (60503, KCLB, oral tongue SCC). FaDu cells were cultured in minimum essential medium (11095-080, Gibco, Life Technologies) medium supplemented with 10% fetal bovine serum (FBS; 6000-044, Gibco; Life Technologies) and 100 U/mL penicillin/streptomycin. SNU-1066, SNU-1076, and YD-10B cells were maintained in Dulbecco's modified Eagle's medium (11995-065, Gibco) with 10% FBS and 100 U/mL penicillin/streptomycin.

2. NOVA1 overexpression

NOVA1 overexpression was induced by transfecting cells with the pCMV-NOVA1 plasmid (SC111659, ORIGENE) using Lipofectamine 3000 transfection reagent (Thermo Fisher Scientific) according to the manufacturer's instructions. Cells were cultured for 24 and 48 hours post-transfection, after which RNA and protein were extracted for analysis.

3. Transfection of poly(dA:dT)

Synthetic double-stranded poly(dA:dT) DNA (tlrl-patn, InvivoGen) was transfected into each cell line at concentrations of 0, 50, and 100 ng/mL, following transfection with the NOVA1-expressing vector. Cells were harvested after 24 and 48 hours of culture for RNA and protein isolation. Each experiment was conducted independently at least three times.

4. RNA isolation and quantitative real-time polymerase chain reaction

Total mRNA was isolated using the RNeasy Plus Mini Kit (74134, Qiagen), and cDNA was synthesized with the SensiFAST cDNA Synthesis Kit (BIO-65054, Meridian Bioscience). Quantitative real-time polymerase chain reaction was conducted using the SensiFAST SYBR Lo-Rox Kit (BIO-94020, Meridian Bioscience) on the Applied Biosystems QuantStudio Real-Time PCR System (Thermo Fisher Scientific). The PCR conditions included an initial denaturation at 95°C for 2 minutes, followed by 40 cycles of 95°C for 15 seconds and 60°C for 1 minute. Primers used are listed in S2 Table. All experiments were performed independently at least three times.

5. Western blot analysis

Cells were lysed using RIPA buffer with a protease/phosphatase inhibitor cocktail, and protein concentrations were measured using a protein quantification kit (Biomax). Proteins from the lysates were separated by electrophoresis on Q-PAGE TGN Precast Gels (QP4520, SMOBIO Technology) and transferred onto polyvinylidene fluoride membranes (Millipore). The membranes were then blocked with 5% bovine serum albumin in Tris-buffered saline with Tween-20 for 1 hour at room temperature. After blocking, membranes were incubated overnight at 4°C with primary antibodies, followed by 2-hour incubation at room temperature with horseradish peroxidase-conjugated secondary antibodies. Protein bands were detected using enhanced chemilumines-

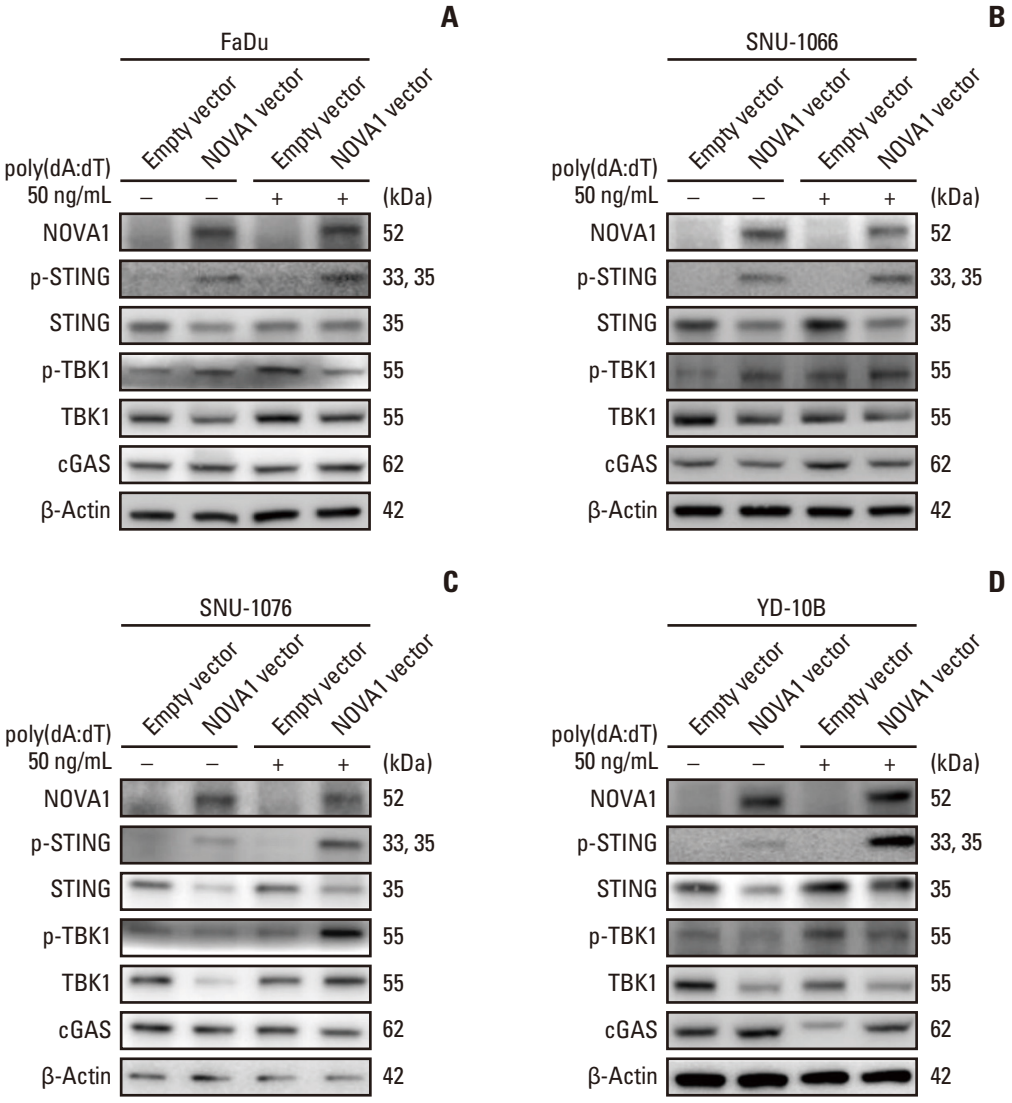

Fig. 1. Protein expression of cGAS-STING pathway molecules following NOVA1 overexpression. The protein expression levels of cGAS-STING pathway molecules were assessed by western blot in FaDu (A), SNU-1066 (B), SNU-1076 (C), and YD-10B cells (D).

cence reagent (ATTO). Details of the primary antibodies are provided in S3 Table.

6. Enzyme-linked immunosorbent assay (ELISA)

Protein levels of CCL5 and CXCL10 in the culture supernatant were quantified using the CCL5 Human RANTES ELISA Kit (ELK1179) and the CXCL10 Human Interferon Gamma-Induced Protein 10 kDa ELISA Kit (ELK1278) from ELK Biotechnology (Wuhan, China), following the manufacturer's instructions.

7. Immunoprecipitation

Cell lysates were incubated with anti-NOVA1 and anti-STING antibodies using Pierce Protein A/G resin (Thermo Fisher Scientific). The procedure was independently repeated at least three times. The precipitated proteins were then analyzed by immunoblotting with anti-NOVA1, anti-p-STING, and anti-STING antibodies. Details of the antibodies used are provided in S3 Table.

8. Clinical samples and immunohistochemistry

Archived formalin-fixed, paraffin-embedded specimens were obtained from patients who underwent curative surgical resection for HNSCC at Severance Hospital, Seoul, Korea. A total of 234 cases were selected from consecutive surgical resections based on the availability of tumor tissue, clinical

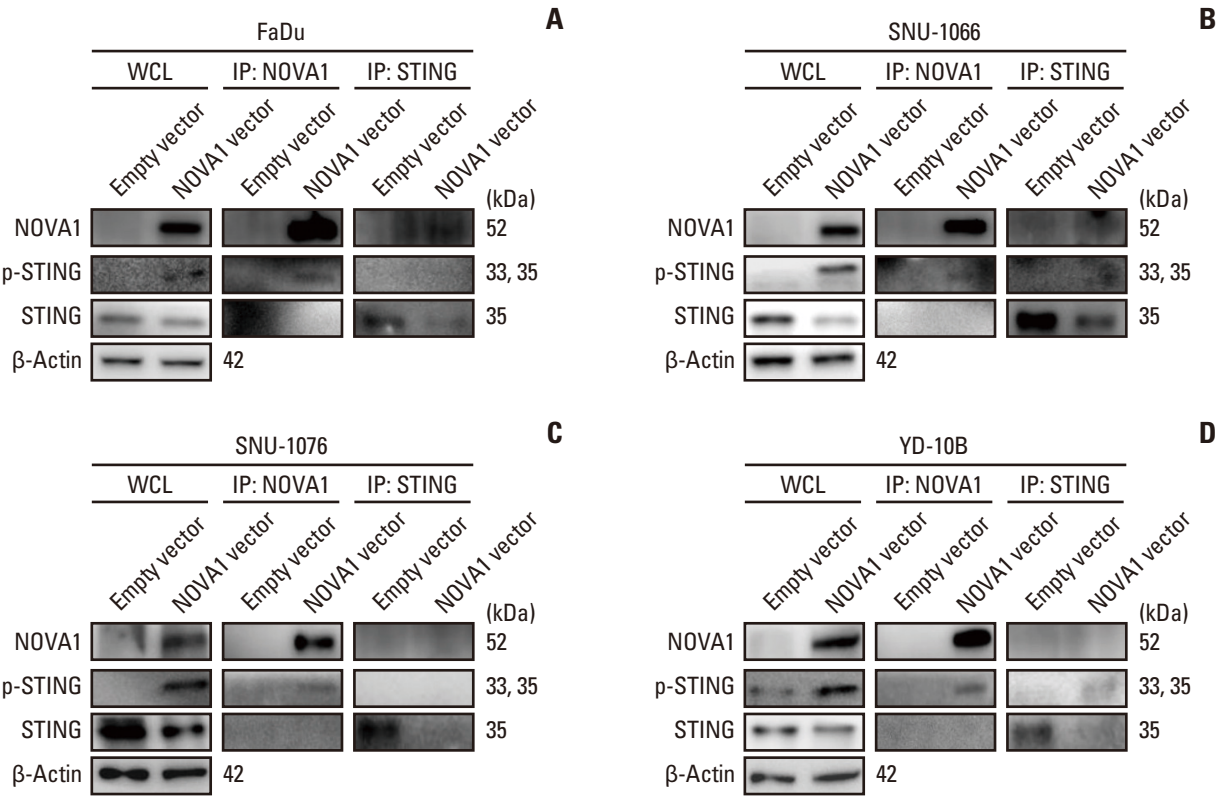

Fig. 2. Interaction between NOVA1 and STING, and between NOVA1 and p-STING. The interactions between NOVA1 and STING, as well as between NOVA1 and p-STING, were analyzed using immunoprecipitation in FaDu (A), SNU-1066 (B), SNU-1076 (C), and YD-10B cells (D).

survival data, absence of preoperative treatments, and no evidence of distant metastasis at the time of surgery. Samples that had undergone decalcification were excluded to ensure accurate immunohistochemical analysis.

Tumor microarrays were constructed using representative formalin-fixed, paraffin-embedded tissues, and immunohistochemistry (IHC) was performed using the antibodies listed in S3 Table on the Benchmark XT autostainer (Ventana Medical Systems) and a LEICA BOND-III Autostainer (Leica Biosystems) according to the manufacturers' protocols. Slides were scanned using an Aperio AT2 slide scanner (Leica Biosystems) at 40× magnification, with a resolution of 0.5 μm per pixel and image thickness of 3.5 μm. Positive cells expressing NOVA1, STING, and p-STING were quantified using QuPath analysis [14]. Regions of interest (ROIs) were manually annotated on representative tumor areas based on hematoxylin and eosin morphology and included both tumor nests and adjacent stroma. For each ROI, the composite positivity index (CPI) was calculated as the percentage of positive cells among all nucleated cells, regardless of cell type. Thus, CPI represents the overall proportion of cells expressing each marker within the ROI. For clinicopathologic and survival analyses, patients were dichotomized into high and low expression groups for each marker, based on optimal cutoff values determined by maximally selected rank statistics, which identify the threshold that most significantly discriminates survival outcomes. In addition, tumor-infiltrating immune cells were quantified to assess immune contexture. In this study, tumor-infiltrating immune cells were defined broadly as all immune cells infiltrating the tumor area, regardless of whether they were located within tumor nests (intratumoral) or in the peritumoral stroma. Quantification of $CD3^+$ and $CD8^+$ T cells was based on previously published data [13], while $FOXP3^+$ regulatory T cells, programmed death-1 $(PD\text{-}1)^+$ tumor-infiltrating lymphocytes (TILs), and $CD163^+$ tumor-associated macrophages (TAMs) were newly analyzed in this study using the same methodology as in the previous work [13].

9. Statistical analysis

Continuous variables were analyzed using an unpaired, two-tailed Student's t test and one-way analysis of variance (ANOVA), followed by Dunnett's multiple comparison test. Bivariate correlation was assessed using Pearson's correla-

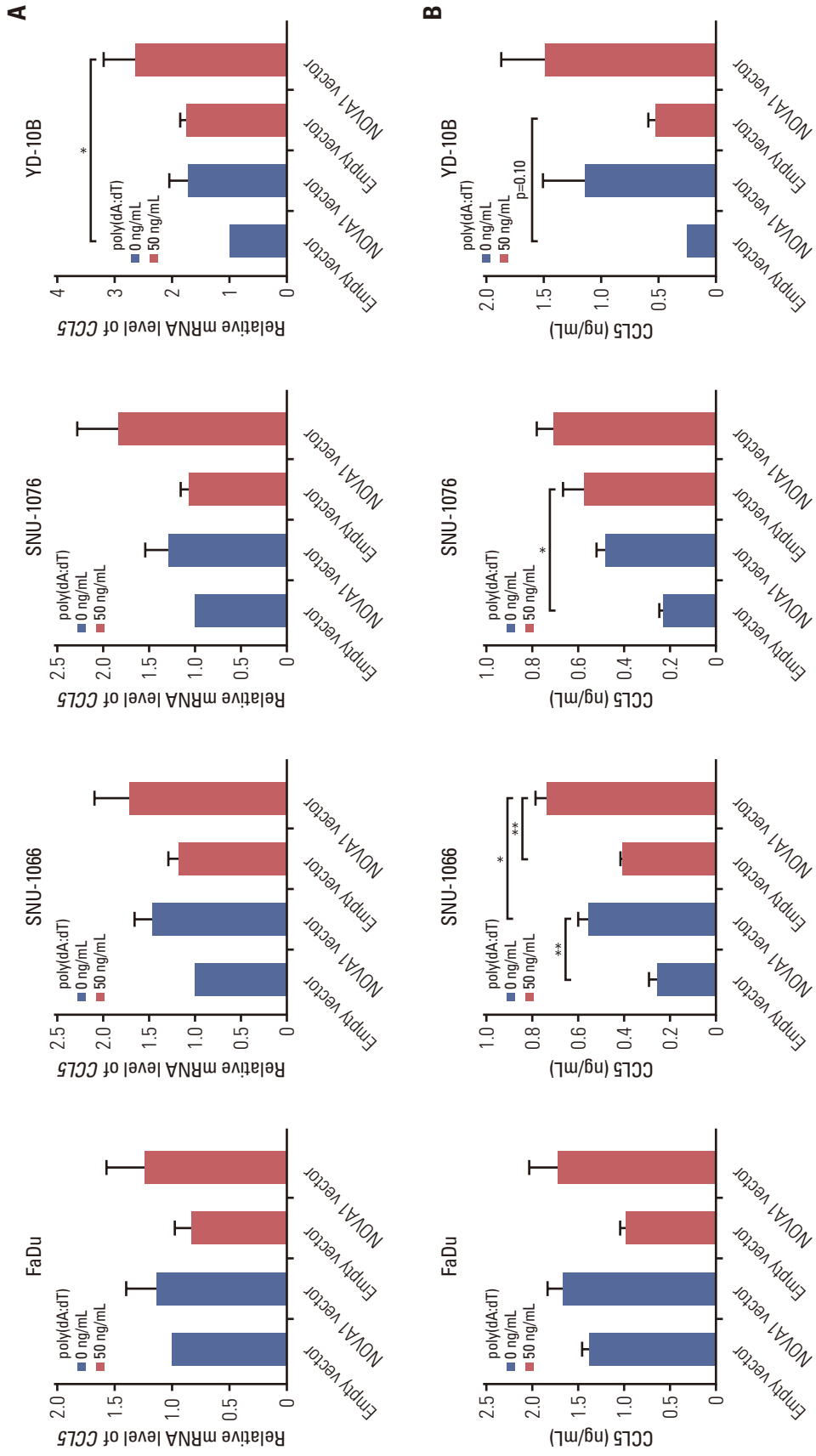

Fig. 3. mRNA and secreted protein levels of C-C motif chemokine ligand 5 (CCL5) and C-X-C motif chemokine ligand 10 (CXCL10) following NOVA1 overexpression. The mRNA and secreted protein levels of CCL5 (A, B) and CXCL10 (C, D) were measured in head and neck squamous cell carcinoma cell lines after NOVA1 overexpression using quantitative real-time polymerase chain reaction and enzyme-linked immunosorbent assay. NOVA1 expression was confirmed by western blot (S4 Fig.). *(Continued to the next page)*

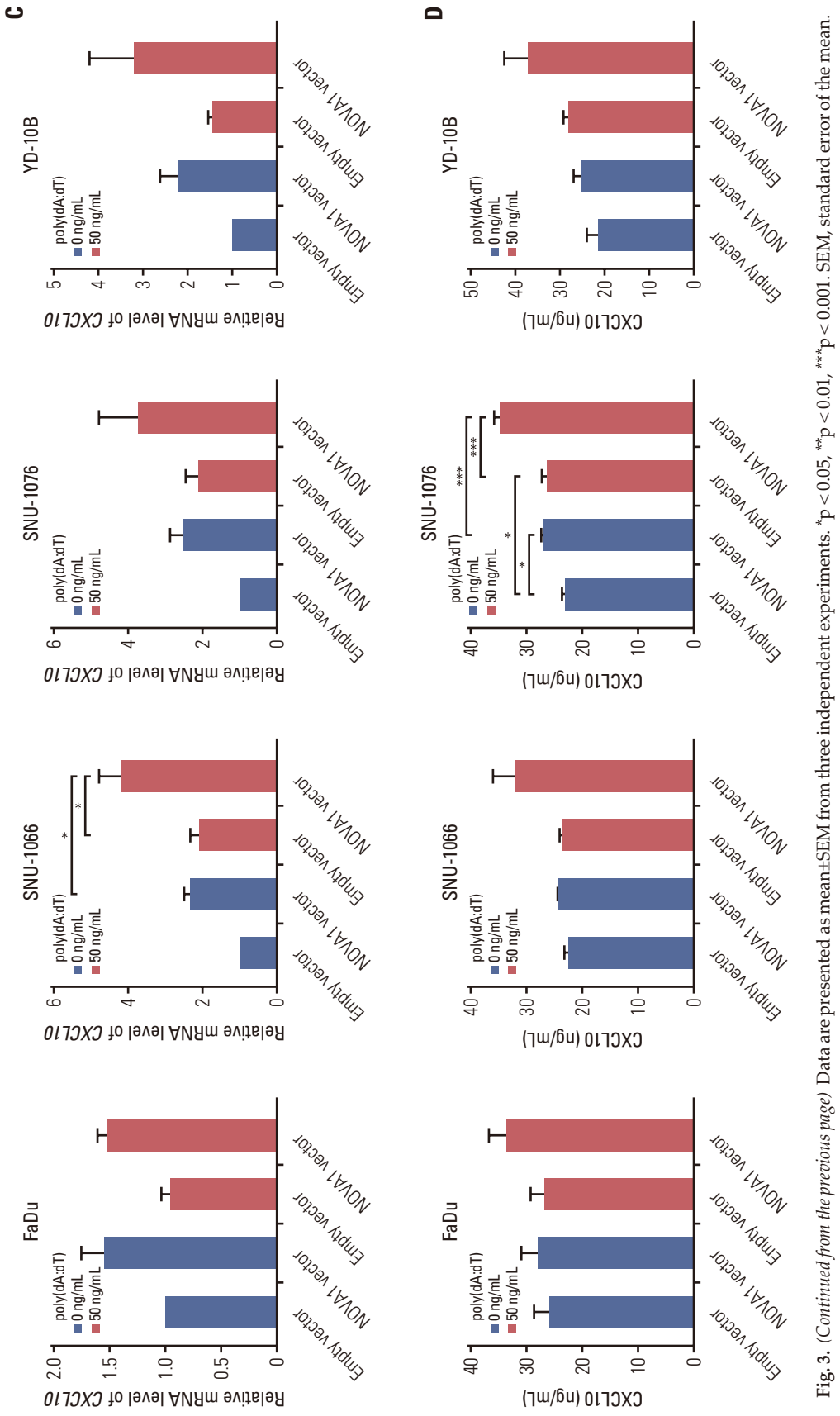

Fig. 3. *(Continued from the previous page)* Data are presented as mean±SEM from three independent experiments. $^{*}p < 0.05$, $^{**}p < 0.01$, $^{***}p < 0.001$. SEM, standard error of the mean.

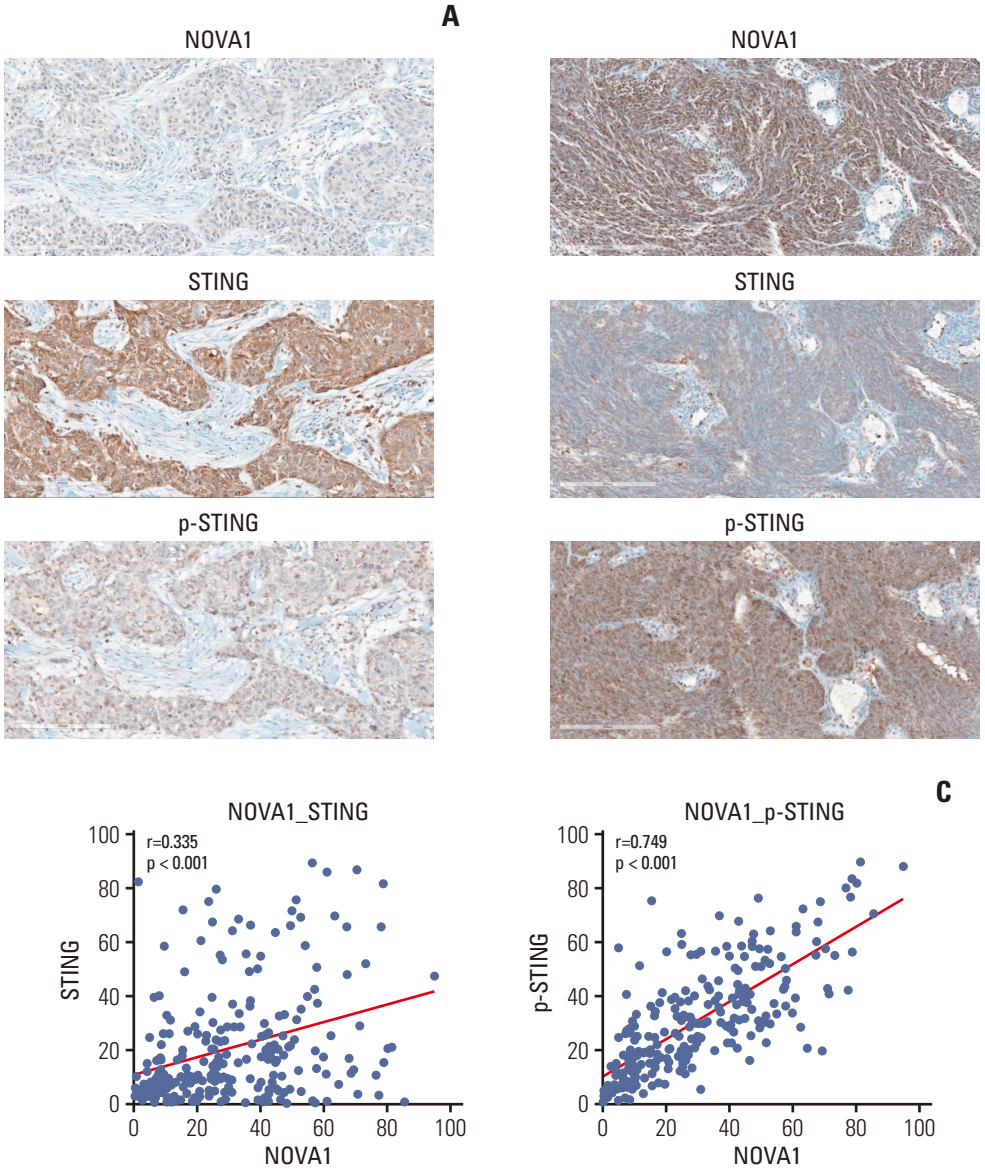

Fig. 4. Correlation between NOVA1, STING, and p-STING expression in head and neck squamous cell carcinoma (HNSCC) clinical samples. Representative immunohistochemistry (IHC) images showing the expression of NOVA1, STING, and p-STING in tumor cells and tumor-infiltrating lymphocytes (TILs) from two HNSCC patient cases (A, B). In case A, NOVA1 and p-STING expression levels were low (composite positivity index [CPI], 23.7% and 17.5%, respectively), whereas STING expression was high (CPI, 75.3%). Conversely, in case B, NOVA1 and p-STING expression levels were high (CPI, 95.0% and 88.2%, respectively), while STING expression was relatively lower (CPI, 47.6%). Images were captured at ×200 magnification. Correlation analysis of CPI levels for NOVA1, STING, and p-STING in tumor cells and TILs (C). A strong positive correlation was observed between NOVA1 and p-STING expression ($r=0.749$, $p < 0.001$), which was notably stronger than the correlation between NOVA1 and total STING expression ($r=0.335$, $p < 0.001$).

tion. A two-sided p-value of less than 0.05 was considered statistically significant. All statistical analyses were performed using SPSS ver. 21 (IBM Corp.) and GraphPad Prism 9 (GraphPad Software).

Results

1. Impact of NOVA1 overexpression on STING pathway modulation in HNSCC cells

Successful NOVA1 overexpression was observed following transfection of the NOVA1 gene into HNSCC cell lines

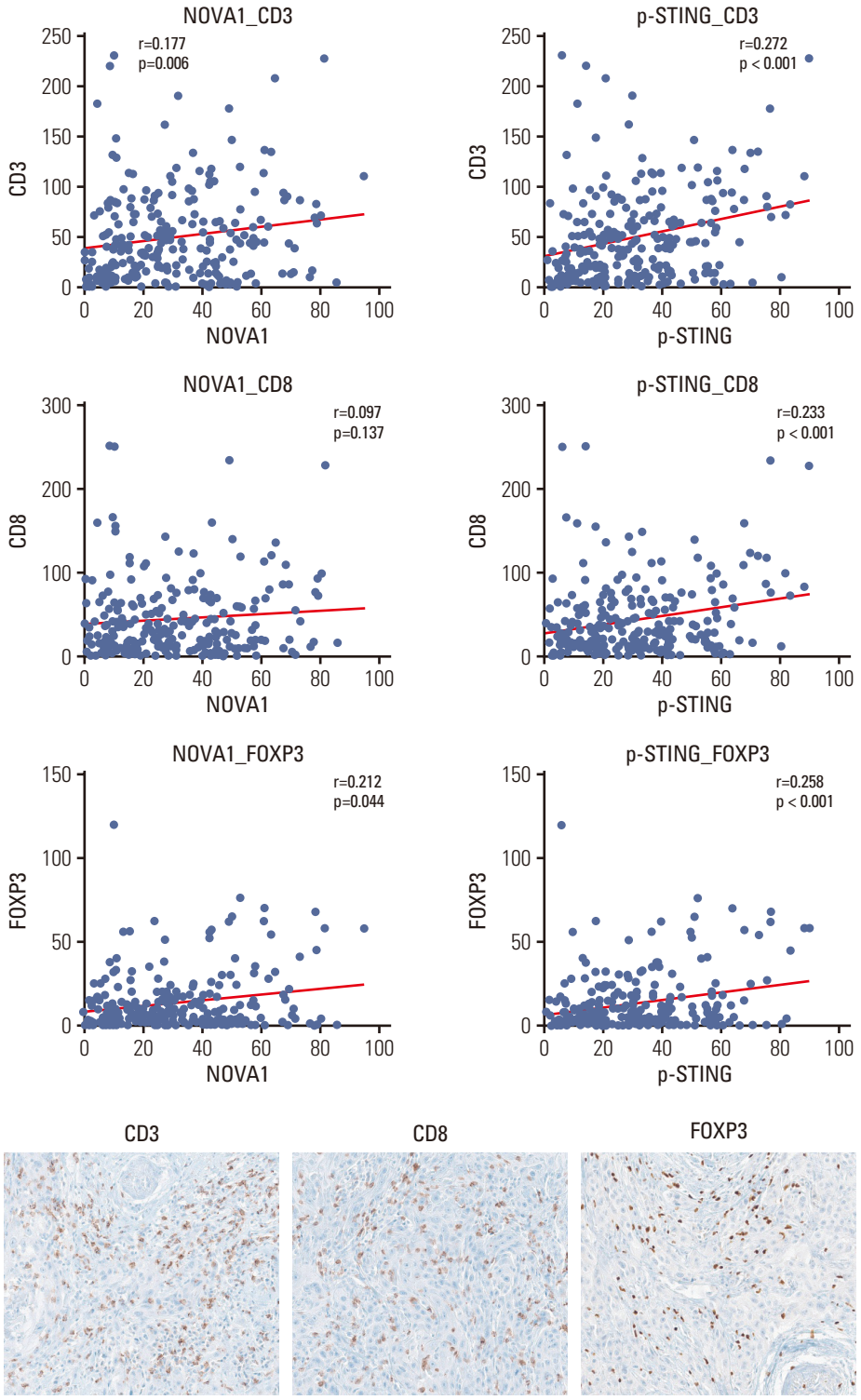

Fig. 5. Correlation between NOVA1 and p-STING expression with T cell subsets. The first row illustrates the correlation between NOVA1 expression and tumor-infiltrating lymphocytes (TILs), including $CD3^+$, $CD8^+$, and $FOXP3^+$ cells. The second row presents the correlation between p-STING and these TIL populations. Composite positivity index levels of NOVA1 and p-STING, along with TIL counts, were assessed using immunohistochemistry (IHC) and automated quantification. The third row displays representative IHC images of $CD3^+$, $CD8^+$, and $FOXP3^+$ T cells.

FaDu, YD-10B, SNU-1066, and SNU-1076 (Fig. 1). Based on our preliminary findings suggesting that NOVA1 may positively regulate the cGAS–STING pathway, we used a suboptimal concentration of poly(dA:dT) to avoid full stimulation of the pathway, which could potentially mask the effect of NOVA1. Notably, the addition of poly(dA:dT) did not significantly affect NOVA1 protein expression (Fig. 1). In NOVA1-overexpressing cells, an increase in p-STING protein was observed, accompanied by a decrease in total STING protein levels. This pattern was notably present in the YD-10B, SNU-1066, and SNU-1076 cell lines. In contrast, NOVA1 overexpression did not affect the expression levels of cGAS, TBK1, or p-TBK1 (Fig. 1). These findings suggest that NOVA1 selectively enhances STING phosphorylation.

2. NOVA1 interaction with phosphorylated STING in HNSCC cells

Immunoprecipitation experiments were conducted to investigate the interaction between NOVA1 and p-STING. As shown in Fig. 2, NOVA1 specifically binds to p-STING, but not to unphosphorylated STING. This interaction was particularly prominent in YD-10B cells. These results suggest that NOVA1 may be involved in the phosphorylation of STING within the cGAS-STING signaling pathway.

3. Increased CCL5 and CXCL10 expression in NOVA1-overexpressing cells with poly(dA:dT) treatment

In NOVA1-overexpressing cells (S4 Fig.), a trend toward increased mRNA levels of *CCL5* and *CXCL10* was observed, with particularly strong effects in YD-10B cells and SNU-1066 cells (Fig. 3A and C). ELISA results showed that CCL5 and CXCL10 secretion tended to be higher in NOVA1-overexpressing cells, and was further elevated with poly(dA:dT) treatment, especially in SNU-1066 and SNU-1076 cells (Fig. 3B and D).

4. Association of NOVA1 with STING phosphorylation and prognostic significance in HNSCC clinical samples

Given the observed effects of NOVA1 on STING phosphorylation and chemokine induction *in vitro*, we next evaluated whether similar associations could be observed in patient tissues. We evaluated the percentage of positive cells for NOVA1, STING, and p-STING proteins in both tumor cells and TILs, based on immunohistochemical analysis of clinical samples from 234 HNSCC patients. Representative IHC images are shown in Fig. 4A and B.

NOVA1 expression did not show a significant association with clinicopathologic parameters (S5 Table). Low p-STING expression tended to be associated with perineural invasion (p=0.075) and was significantly related to advanced T stage, particularly T4 (when grouped as T1-3 vs. T4, p=0.027) (S6 Table). Additionally, low total STING expression was significantly associated with p16 negativity and high tumor budding (≥ 10) ($p < 0.001$ and p=0.021, respectively) (S7 Table).

In survival analysis, low NOVA1 expression was significantly associated with poor progression-free survival (PFS) (p=0.036) (S8 Fig.). Similarly, reduced expression of p-STING was significantly linked to both poor PFS (p=0.003) and overall survival (OS) (p=0.010), while low STING expression was associated with poor PFS (p=0.041) and showed a non-significant trend toward worse OS (p=0.066). These associations were even more pronounced in the oropharyngeal SCC subgroup, where low expression of NOVA1, p-STING, and STING were each significantly correlated with both inferior PFS and OS (NOVA1: PFS, p=0.006; OS, p=0.023; p-STING: PFS, p=0.004; OS, p=0.023; STING: PFS, p=0.004; OS, p=0.007) (S8 Fig.).

Importantly, correlation analysis revealed a strong positive association between NOVA1 and p-STING protein expression ($r=0.749$, $p < 0.001$), which was markedly stronger than the correlation between NOVA1 and total STING expression ($r=0.335$, $p < 0.001$) (Fig. 4C). This finding not only supports our *in vitro* results but also reinforces the notion that NOVA1 may specifically modulate the phosphorylation status of STING rather than its overall expression. The consistency of this association across patient-derived tumor tissues further strengthens the clinical relevance of the NOVA1–p-STING axis in shaping the immune microenvironment and influencing prognosis in HNSCC.

5. Correlation between p-STING and NOVA1 expression and tumor-infiltrating immune cells

To determine whether the immune-activating effects of NOVA1 observed *in vitro* are reflected in patient tissues, we analyzed the correlation between NOVA1, p-STING, and immune cells in clinical samples. Elevated p-STING expression was significantly correlated with higher infiltration of tumor-infiltrating $CD3^+$ T cells ($r=0.272$, $p < 0.001$), $CD8^+$ T cells ($r=0.233$, $p < 0.001$), and $FOXP3^+$ regulatory T cells (Tregs) ($r=0.258$, $p < 0.001$). Similarly, higher NOVA1 expression was associated with increased infiltration of $CD3^+$ T cells ($r=0.177$, p=0.006) and $FOXP3^+$ Tregs ($r=0.212$, p=0.044), although these correlations were weaker than those observed for p-STING (Fig. 5). Additionally, both NOVA1 and p-STING expression levels were positively correlated with $PD\text{-}1^+$ TILs, indicative of activated lymphocytes (NOVA1: $r=0.185$, p=0.034; p-STING: $r=0.300$, $p < 0.001$) (S9 Fig.). In contrast, p-STING expression, but not NOVA1 expression, showed a weak but statistically significant correlation with $CD163^+$ TAMs, which are typically associated with an immunosuppressive M2-like phenotype (p-STING: $r=0.135$, p=0.038; NOVA1: $r=0.021$, p=0.744) (S9 Fig.). These findings support

the association of NOVA1 with a more immune-active tumor microenvironment, potentially through its role in modulating STING phosphorylation and downstream T-cell recruitment.

Discussion

This study highlights the role of NOVA1 in regulating the cGAS-STING immune-inflammatory pathway in HNSCC, with potential implications for anti-tumor immunity. Our findings suggest that NOVA1 modulates the phosphorylation of STING, leading to an immune response characterized by the secretion of chemokines such as CCL5 and CXCL10, and increased infiltration of proinflammatory immune cells, including $CD3^+$ T cells and $PD\text{-}1^+$ TILs.

Overexpression of NOVA1 in HNSCC cell lines resulted in a marked increase in p-STING, without altering the levels of cGAS or TBK1 proteins, both of which are key components in the activation of the cGAS-STING pathway. This selective modulation indicates that NOVA1 specifically interacts with phosphorylated STING.

While NOVA1 is primarily known as an alternative splicing factor that functions at the post-transcriptional level, our data imply a novel role in modulating post-translational events, particularly STING phosphorylation. NOVA1 expression did not affect TBK1 phosphorylation and selectively bound to p-STING. Additionally, no changes were observed in cGAS or TBK1 protein levels. Although the exact mechanism remains unclear, NOVA1 may promote STING phosphorylation either through direct interaction or via yet unidentified upstream regulators outside the canonical cGAS-STING pathway. These findings suggest a potentially novel and complex regulatory relationship between NOVA1 and STING activity that warrants further mechanistic investigation.

In our study, p-STING expression was significantly associated with increased infiltration of proinflammatory T cell subsets, including $CD8^+$ T cells and $PD\text{-}1^+$ TILs, as well as $FOXP3^+$ Tregs. $CD8^+$ T cells are key mediators of anti-tumor immunity, while $FOXP3^+$ Tregs suppress excessive immune activation to maintain immune homeostasis. The concurrent increase in $FOXP3^+$ Tregs alongside proinflammatory T cells may reflect a compensatory response to heightened immune activation, as has been previously observed in inflamed tumor microenvironments [6,8,15]. NOVA1 expression, like p-STING, was positively associated with $CD3^+$ T cells and $PD\text{-}1^+$ TILs, supporting its potential role in promoting a proinflammatory immune context. While the correlation between NOVA1 and $CD8^+$ T cells was not statistically significant, the overall pattern was largely consistent with that of p-STING.

Supporting this, our *in vitro* experiments demonstrated that NOVA1 overexpression enhanced STING phosphorylation and was accompanied by a trend toward elevated CCL5 and CXCL10 expression—key chemokines known to recruit T cells into the tumor microenvironment. Although STING inhibition experiments were not conducted to confirm its necessity in this study, the observed link between NOVA1 expression, STING phosphorylation, and T cell–recruiting chemokines suggests that STING-dependent signaling may underlie the immune-modulating effects of NOVA1.

Taken together, our findings suggest that NOVA1 contributes to an immune-active tumor microenvironment in HNSCC, likely through the enhancement of STING phosphorylation and subsequent chemokine-mediated T cell recruitment. Although its effects were less pronounced than those of p-STING, NOVA1 may act as an upstream regulator with potential relevance for tumor immunobiology and therapeutic targeting.

The cGAS-STING pathway is a promising target in cancer immunotherapy, with several STING agonists undergoing clinical evaluation for their ability to boost anti-tumor immunity [16,17]. However, its complex role in immune regulation necessitates context-dependent modulation [17,18]. In this study, NOVA1 emerged as a potential upstream modulator of STING phosphorylation, with effects on chemokine production and T cell recruitment. These findings raise the possibility that NOVA1 could be further explored as a novel biomarker or regulatory target in strategies aiming to optimize STING-driven anti-tumor responses.

In summary, we demonstrate that NOVA1 modulates STING phosphorylation and contributes to a more immune-active tumor microenvironment in HNSCC. By linking an RNA-binding protein to innate immune signaling, our findings offer new insight into tumor immunoregulation and suggest a potential role for NOVA1 in future immunotherapeutic approaches.

Electronic Supplementary Material

Supplementary materials are available at Cancer Research and Treatment website (https://www.e-crt.org).

Ethical Statement

This work was approved by the Institutional Review Board of Severance Hospital, Yonsei University Health System (4-2021-1561). Informed consent was waived due to the retrospective nature of the study involving no direct patient contact.

Author Contributions

Conceived and designed the analysis: Kim S, Yoon SO.
Collected the data: Kim S, Yoon SO.

Contributed data or analysis tools: Kim S, Yoon SO.
Performed the analysis: Kim S, Kim HM, Bae JM, Yoon SO.
Wrote the paper: Kim S, Bae JM, Yoon SO.

ORCID iDs
Sehui Kim : https://orcid.org/0000-0002-6640-3051
Sun Och Yoon : https://orcid.org/0000-0002-5115-1402

Conflicts of Interest
Conflict of interest relevant to this article was not reported.

Funding
This work was supported by a National Research Foundation of Korea grant funded by the Korean government (Ministry of Science and ICT) (No. NRF-2019R1A2C1002370).

References

1. Barash Y, Calarco JA, Gao W, Pan Q, Wang X, Shai O, et al. Deciphering the splicing code. Nature. 2010;465:53-9.
2. Kalsotra A, Cooper TA. Functional consequences of developmentally regulated alternative splicing. Nat Rev Genet. 2011;12:715-29.
3. Mallinjoud P, Villemin JP, Mortada H, Polay Espinoza M, Desmet FO, Samaan S, et al. Endothelial, epithelial, and fibroblast cells exhibit specific splicing programs independently of their tissue of origin. Genome Res. 2014;24:511-21.
4. Meldolesi J. Alternative splicing by NOVA factors: from gene expression to cell physiology and pathology. Int J Mol Sci. 2020;21:3941.
5. Li T, Chen ZJ. The cGAS-cGAMP-STING pathway connects DNA damage to inflammation, senescence, and cancer. J Exp Med. 2018;215:1287-99.
6. Gan Y, Li X, Han S, Liang Q, Ma X, Rong P, et al. The cGAS/STING pathway: a novel target for cancer therapy. Front Immunol. 2021;12:795401.
7. Gao M, He Y, Tang H, Chen X, Liu S, Tao Y. cGAS/STING: novel perspectives of the classic pathway. Mol Biomed. 2020;1:7.
8. Kaneta A, Nakajima S, Okayama H, Matsumoto T, Saito K, Kikuchi T, et al. Role of the cGAS-STING pathway in regulating the tumor-immune microenvironment in dMMR/MSI colorectal cancer. Cancer Immunol Immunother. 2022;71:2765-76.
9. Chen Q, Sun L, Chen ZJ. Regulation and function of the cGAS-STING pathway of cytosolic DNA sensing. Nat Immunol. 2016;17:1142-9.
10. Motwani M, Pesiridis S, Fitzgerald KA. DNA sensing by the cGAS-STING pathway in health and disease. Nat Rev Genet. 2019;20:657-74.
11. Kang J, Wu J, Liu Q, Wu X, Zhao Y, Ren J. Post-translational modifications of STING: a potential therapeutic target. Front Immunol. 2022;13:888147.
12. Kim EK, Yoon SO, Jung WY, Lee H, Kang Y, Jang YJ, et al. Implications of NOVA1 suppression within the microenvironment of gastric cancer: association with immune cell dysregulation. Gastric Cancer. 2017;20:438-47.
13. Kim EK, Cho YA, Seo MK, Ryu H, Cho BC, Koh YW, et al. NOVA1 induction by inflammation and NOVA1 suppression by epigenetic regulation in head and neck squamous cell carcinoma. Sci Rep. 2019;9:11231.
14. Bankhead P, Loughrey MB, Fernandez JA, Dombrowski Y, McArt DG, Dunne PD, et al. QuPath: Open source software for digital pathology image analysis. Sci Rep. 2017;7:16878.
15. Zheng J, Mo J, Zhu T, Zhuo W, Yi Y, Hu S, et al. Comprehensive elaboration of the cGAS-STING signaling axis in cancer development and immunotherapy. Mol Cancer. 2020;19:133.
16. Sivick KE, Desbien AL, Glickman LH, Reiner GL, Corrales L, Surh NH, et al. Magnitude of therapeutic STING activation determines CD8(+) T cell-mediated anti-tumor immunity. Cell Rep. 2018;25:3074-85.
17. Tian Z, Zeng Y, Peng Y, Liu J, Wu F. Cancer immunotherapy strategies that target the cGAS-STING pathway. Front Immunol. 2022;13:996663.
18. Jiang M, Chen P, Wang L, Li W, Chen B, Liu Y, et al. cGAS-STING, an important pathway in cancer immunotherapy. J Hematol Oncol. 2020;13:81.